Design of a High-Temperature Camera Housing

Dustin M. Gohmert, Peter P. Meier

Mechanical Engineering Department
University of Texas at San Antonio

Abstract

A high temperature camera housing has been designed at the Mechanical Engineering Department at the University of Texas at San Antonio. This paper documents the design, analysis, construction, and demonstration of a camera housing rated for use in high temperature environments up to 2000°F. To design the camera housing, the operating temperature range for the camera was established and energy balance equations were applied to ensure that the radiation shielding and mass flow rate of the cooling air and water were sufficient to remove the heat load of the furnace. In addition head loss was calculated to ensure proper water flow from ordinary faucet connections and operating pressures. Finally, the camera housing was manufactured and tested at Southwest Research Institute (SwRI), located in San Antonio Texas, to validate design performance. All design criteria were met and the camera is currently employed for use in all furnace tests at SwRI.

Introduction

The housing is designed to allow a surveillance camera to be mounted within a test furnace at Southwest Research Institute's Department of Fire Technology. Motivation for this project arises from the need to view test samples while under extreme fire exposure. High temperature housings similar to the proposed design are currently available, however they range in price from $5,000-10,000. The goal of this project was to produce a high-temperature camera housing for less than $1000.

In heat transfer, conduction, convection, and radiation must be accounted for in the energy balance equations. The two primary issues for camera operation were heat absorption of the housing shell, and radiative heat transfer to the visible camera lens.

System Specifications

Before design of the camera housing was started, specific design criteria was be established. Based on the temperature operating range of an ordinary surveillance camera, temperature constraints within the camera were specified to be no greater than 120°F (49°C). The camera housing should be removable from the furnace and the camera should also be easily removable from the housing for service and repairs. Water flow through the camera should be such that it can be provided from an ordinary faucet without a pump. Finally, the housing should be limited

in size to no larger than six inches in diameter in order to reduce the overall opening in the furnace wall where the housing is to be mounted.

Design Methodology

To begin work on the furnace camera housing, research was performed to locate current designs of similar high-temperature housings. In review of currently available designs, it was found that the most common approach to transferring heat from the housing was through the use of water – flow through concentric tubes surrounding the camera. This premise was chosen as the basis for this project because of its reliability and relative ease of manufacture. Figure 1, shown below, illustrates the initial concept developed for the camera housing. A series of three concentric tubes surrounds the furnace camera creating two "flow chambers" through which water passes. The camera is placed in a central cavity in the center of the innermost tube. Stainless steel was chosen for construction of the camera housing because of its availability and low coefficient of thermal expansion

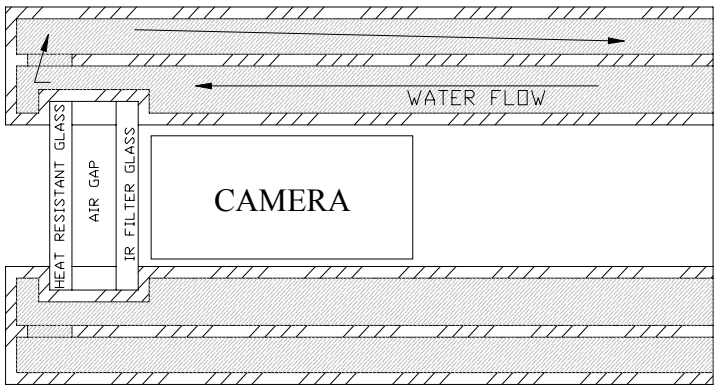

Figure 1. Preliminary Design of Furnace Camera Housing.

From the diagram it is seen that water is introduced inside the middle chamber, reversed in direction at the front of the housing and exited through the outer chamber. The camera is mounted in the center chamber behind a series of heat resistant and infrared absorbing glass. To reduce the effects of radiative heat transfer to the camera through the viewport an infrared filter is employed to block out infrared frequencies emitted over the temperature range of the furnace. To protect the IR filter, a plate of high-temperature resistant glass is positioned as the primary viewport interface between the housing and the furnace.

Heat Load Evaluation

The first step in the analysis was to determine the heat load for the camera housing. To determine, the overall heat flux generated by the furnace was multiplied by the estimated surface area of the camera housing. The heat flux generated by the furnace was known from the calibration of the furnace to various test standards employed at SwRI. The most stringent of the test standards is the Underwriters Laboratory 1709 (UL 1709) which requires a calibrated heat flux generation of up to 70 000 BTU/ ft^2 hr (220 000 kW). The required temperature within the

furnace at the specified heat flux is approximately 2 000°F (1366 K). From these two specifications it is seen that the required heat flux is radiation dominated.

$$Q'' = G'' = E_{burners} = \sigma T_{furnace}^{4} \qquad \text{Eq. 1}$$
$$Q'' = 197\,417 \text{ W/m}^2$$

where σ is the Stefan-Boltzman constant equal to $5.67*10^{-8}$ W/m^2 K^4 and furnace is the furnace wall temperature taken to be the same as the air temperature within the furnace. It should be stated that the measured heat flux during calibration is taken from a calorimeter which only reads the irradiation, G, and neglects the outgoing radiation, J. Therefore, in this instance heat flux is equated only to irradiation. The calculated heat flux accounts for approximately 90% of all heat flux carried by the burners to the calorimeters. Because of the high degree of radiative heat transfer within the furnace it was determined that the radiative shield is necessary to protect the exposed lens of the camera.

Because the calibrated heat flux does not account for radiosity leaving the receiving surface, it is know that heat flux actually seen by the camera will be less than that specified. The assumption of 220 000 W/m^2 was used for the duration of this project as a worst-case scenario estimator.

The surface area of the camera was originally estimated using a tube 6-in. (0.1524 m) diameter and 12-in. (.3048 m) long. The area of the front surface of the tube was also included by taking the area of the diameter surrounding the front glass . The presented calculations will account for the final surface area taken from a 4.5-in. (0.1143m) diameter tube 12-in. (.3048 m) long. From this calculated surface area and the applied heat flux, the calculated heat load is presented in Equation 2, below:

$$Q = Q''A \qquad \text{Eq. 2}$$
$$Q = 25\,322 \text{ W}$$

Mass Flow Rate

Once the applied heat to the camera housing was known, the necessary flow rate of the water to cool the system was calculated from Equation 3:

$$Q = \dot{m}\, c_p\, (T_{out} - T_{in}) \qquad \text{Eq. 3}$$

and rearranged:

$$\dot{m} = Q / [c_p * (T_{out} - T_{in})]$$

where T_{out} is the specified water temperature leaving the camera housing and T_{in} is the estimated supply water temperature. The specific heat of water, c_v, was held constant at 4180 J/kg K since the change in c_v is minimal in the water operating range. The water temperature exiting the camera housing was held to a 20 K change in order to keep the temperature of the camera housing as low as possible. The temperate change could not be held lower than the specified value because it was found that to do so would require an unobtainable mass flow rate of water through the camera. Finally, from Equation 3, a mass flow rate of 0.384 kg/s was calculated. Converted to volumetric flow rate, this number equals 6.09 gallons per minute (GPM), a flow

rate easily obtainable from an ordinary faucet connection. An important note to the calculated flow rate is that it is assumed that all heat transfer from the furnace to the water occurs in the outer water chamber.

Reynolds Number

Upon specification of the mass flow rate and tubing sizes the Reynolds number of the flow in the outer chamber was calculated. From the Reynolds number calculations, pressure drop of the water flow and outer surface temperature of the housing can be found. The final specified tubing diameters are as follows:

Table 1. Final Tubing Diameters.

Inner Tube		Middle Tube		Outer Tube	
Outer diameter	Inner diameter	Outer diameter	Inner diameter	Outer diameter	Inner diameter
3.5	3.068	4	3.875	4.5	4.375

From these diameters and the mass flow rate, areas and velocity through the inner and outer water flow cavities are found and are presented in Table 2.

Table 2. Flow Chamber Data.

Chamber	Inner	Outer
Height (mm)	9.5	9.5
Area (mm^2)	0.0014	0.0016
Velocity (m/s)	0.2742	0.2414

Since the majority heat transfer is assumed to occur the space between the middle and outer tubes, Reynolds numbers and further calculations are presented only in this area. To calculate Reynolds number, Re, Equation 4 was used:

$$Re = \rho V D / \mu \qquad \text{Eq. 4}$$

where ρ is the density of the fluid, V is velocity of the fluid, D is the hydraulic diameter of the chamber, and μ is the viscosity. Hydraulic diameter is defined as the outer diameter minus the inner diameter. A Reynolds number of 3731 was calculated, which signifies that the flow through the outer chamber is located in the transition zone between laminar and turbulent flow. Attempts were made to size the tubes accordingly to raise Re to fully turbulent conditions, however this cannot be accomplished in a concentric tube arrangement as is presented. As hydraulic diameter is increased, flow velocity decreases, thereby causing very little net gain or loss in Re.

It is desired to have high turbulence in flow through the outer flow chamber because the convective heat transfer coefficient is maximized in this region. Since Re is over 2000, flow is definitely not laminar, and since it is approaching the turbulence threshold of 4000, the

assumption of turbulence was made for the remainder of the project. This is valid assumption since turbulence will be introduced by the 180° bend the flow must pass through. In addition, spacers are welded at the front of the housing between the middle and outer tubes that act as turbulators as fluid passes around them. Since the length of the housing is only 16 in. it is unlikely that the flow will straighten out, especially in the areas exposed to the furnace.

Exposed Surface Temperature

An important consideration for the construction of the camera housing is the exterior surface temperature. If the temperature rises too high, thermal expansion will cause excessive stress in the outer surface resulting in possible warping and leakage. To find the outer surface temperature the Reynolds number found above was used to calculate the Nusselt number, Nu. The Nusselt number is defined in Equation 5, as follows;

$$Nu = (0.023)\, Re^{4/5} * Pr^{1/3} \qquad \text{Eq. 5}$$
$$Nu = 24.92$$

where Pr is the Praneldt number, which is located from previously tabulated data {1}. The Nusselt number is then used to find the average convective heat transfer coefficient, h. The calculated h was found from Equation 6:

$$h = Nu * (k / D) \qquad \text{Eq. 6}$$
$$h = 1643\ W/m^2K$$

where k is the thermal conductivity of water from heat transfer tables {2}. Knowing h and Q the surface temperature of the camera was found.

$$Q = h\, A(T_{surf} - T_{water\text{-}out}) \qquad \text{Eq. 7}$$

Rearranged to:

$$Tsurf = Q'' / h + T_{water}$$

Equation 7 yields a camera housing surface temperature of 169°C (336°F). The coefficient of expansion, α, for type 304 stainless steel was found to be 0.00001728 m/m°C. By multiplying α $*(\Delta T_{surf})$ it is found that the outer surface will expand only 0.24%; a negligible amount.

In total, all of the above calculations show that the camera and camera housing should maintain their integrity given the prescribed heat exposure. While it would be possible to slightly increase overall performance by sizing the tubes to obtain a higher Reynolds number the design was limited by the available tubing sizes and other considerations of manufacture.

Head Loss

The specified tubes were then checked to see if flow was possible through the given spaces between the tubes and the required flow rate. The major losses and minor losses were calculated using the basic principles from fluid dynamics. The theoretical pressure drop was calculated using the assumption of turbulent flow. The Reynolds number was used with the diameter and

roughness to give a frictions coefficient of 0.04 from the Moody diagram. The loss coefficient K was calculated using Eq. 8.

$$K=L/D \qquad \text{Eq. 8}$$

where L is the length of the water run taken to be 144 inches, which takes into account the 180°, turn and the 24 in. of actual length. D is the hydraulic diameter of the concentric tubes. The velocity of the flow was calculated as shown in Equation 9.

$$V=AV/A \qquad \text{Eq. 9}$$

in which V is velocity, AV is volumetric flow rate, and A is the cross sectional area. Major head loss was then given by Equation 10.

$$Hlm=KV^2/2 \qquad \text{Eq. 10}$$

where Hlm is the head loss. The head loss was calculated to be 0.685 meters. The minor losses from the expansion and contraction of the water entering and leaving the tubes were also calculated using the Loss coefficients for flow through sudden area changes[6] in Equation 11 and Equation 12.

$$Hlm=KcV^2/2 \qquad \text{Eq. 11}$$

$$Hlm=KeV^2/2 \qquad \text{Eq. 12}$$

where Kc is the contraction loss and Ke is the expansion loss coefficient. The values for the loss coefficients are given on Figure 8.15 in Fox {6}. The head loss for contraction was calculated to be 1.65 meter and expansion was 2.47 meters. Adding all head losses up and multiplying by density and gravity gave the pressure drop expected to be 6 psi.

Experimental pressure drop was also calculated. The flow with the camera housing inline was measured several times and the flow without the camera housing inline was also measured. The difference in the two pressure drops was 3.5 psi. The calculated values are reasonably close and point to an overestimation of the losses from the 180° turn and the expansion and contraction losses.

Heating Effects Through Viewport

Because of the high degree of radiative heat transfer at 2000°F, the camera must be shielded from its effects. The front lens of the camera as shown in Figure 1 is a thermal resistant ceramic glass. The product chosen to meet the design requirements is Firelite® Ceramic Glass manufactured by Technical Glass Products, Inc. The function of this glass is to act as a barrier between the camera compartment and the furnace environment. Important qualities of the glass include its high-temperature resistance and its extremely low coefficient of thermal expansion. The low α guarantees that the glass will not shatter from stresses caused by expansion within its housing. A negative attribute of the thermal glass is that it does not act as a barrier to thermal

radiation. Because of this, a second layer of glass, a radiation-absorbing lens, was placed before the camera.

The light emission wavelength vs. temperature chart is shown in Figure 1.

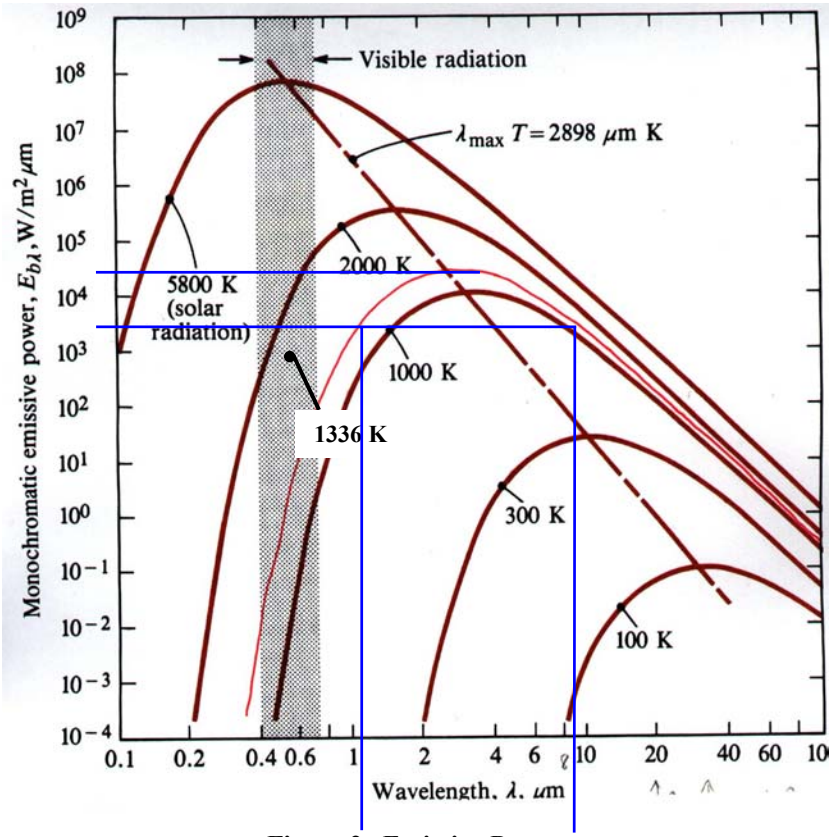

Figure 2. Emissive Power

At 2000°F (1366 K) approximately 90% of the spectral emission at this temperature is concentrated from 1000 to 10,000 nanometers (nm). To stop the effects of radiation from transferring to the camera, the radiation absorbing glass was chosen to block the light frequencies within this region. A Schott KG-1 infrared (IR) radiation absorbing lens was chosen to meet the presented challenge. A seen in Figure 3, the Schott KG-1 glass effectively blocks all light in the infrared region while allowing approximately 90% transmittance of visible light. Visible light transmission is important because otherwise a dim or distorted picture would be recorded by the camera.

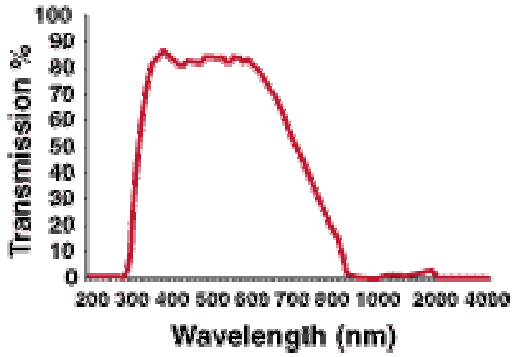

Figure 3. Percent Light Transmission of Schott KG-1 Glass

Infrared-absorbing glass was chosen for the design over infrared-reflecting glass because of its increased filtering range. Because it absorbs incoming radiation, temperature of the glass will rise quickly if not cooled by forced air convection. Temperature of the glass was reduced in two ways in the final design, (1) forced air convection was introduced over the inner surface of the glass, and (2) the overall viewport assembly was recessed into the camera housing 1.5 inches in order to reduce the radiation view factor seen by the glass.

Forced air convection over the IR glass is introduced inside the camera compartment. The airflow not only serves to cool the glass, but to maintain a cool airflow over the camera surface. By receding the camera in the housing, the view factor was reduced, thereby increasing overall resistance to radiative heat transfer. In addition the receded viewport assembly provides a cavity for cooling air to circulate thereby displacing hot gasses of the furnace with cool air. Because of this, effects of convection from the furnace to the front glass can be neglected. The forced air displacement also serves to protect the front glass from soot and other debris that could accumulate over time and obscure the recording.

Uncertainty Analysis

Uncertainty analysis was performed on the major calculation in the project shown in Equation 13.

$$Q=\dot{m}c_p(To-Ti) \qquad \text{Eq. 13}$$

Rearranged to

$$\dot{m} =Q/(c_p*(To-Ti)$$

The uncertainty was calculated assuming a temperature of ± 0.5 °C, cp ± 20, and Q ± 200. The uncertainty in the mass flow came out to be 10% using Equation 14.

$$\dot{m}_{uncert} = \sqrt{\left(\frac{\delta \dot{m}}{\delta Q}\Delta Q\right)^2 + \left(\frac{\delta \dot{m}}{\delta c_p}\Delta c_p\right)^2 + \left(\frac{\delta \dot{m}}{\delta T}\Delta T\right)^2} \qquad \text{Eq. 14}$$

Final Design

The final design of the camera housing is shown in Figure 4. The heat resistant glass and IR-absorbing glass are fastened in stainless steel mounts to reduce their size and cost. The mounts also allow for the front air line to pass through a notch cut in the outer diameter of the mount. Between the thermal-resistant glass and the IR-absorbing glass two layers of 2 mm thick insulating board was fit. The low thermal conductivity of the insulating board lowered the effects of conduction through the viewport assembly. The insulating board also has a low emissivity, thereby further reducing effects of radiation.

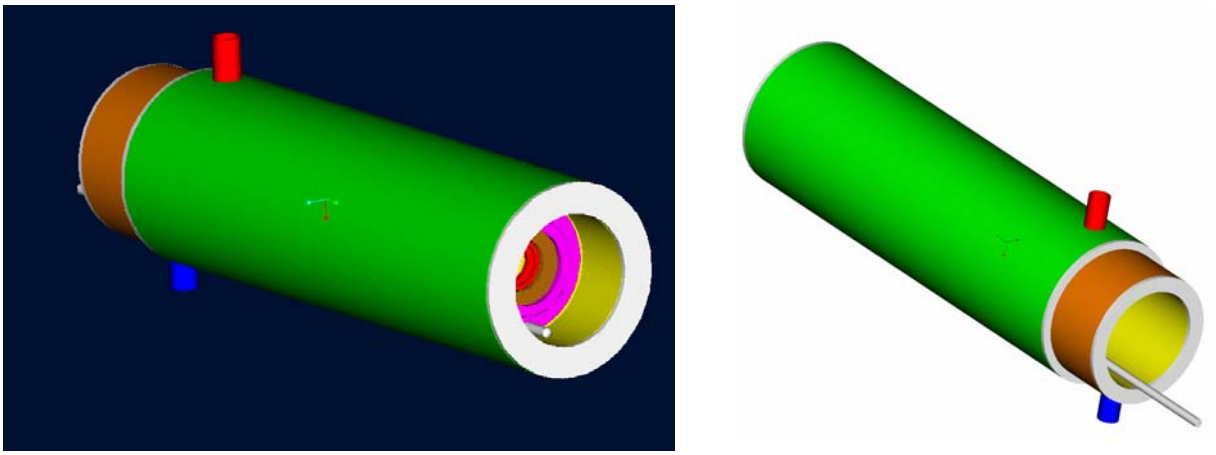

Figure 4. 3-Dimensional Representation of Camera Housing.

To hold the viewport assembly and the camera mounting plate, notches were cut in the inner walls of the housing to accommodate snap rings. The snap rings allow for easy removal of all components within the camera housing while maintaining a firm connection during use. A common 0.25 in. plastic air tube is split to provide the cooling air over the front glass as well as the IR-absorbing glass. From experimental data gathered at SwRI it was determined that a pressure of 30 psi would provide sufficient airflow to displace hot air and cool the camera as needed.

Manufacture and Total Cost

Final design drawings were generated showing all views of the camera housing and all components necessary for fabrication. All steel used in the camera housing was T304 Stainless Steel. The manufactured camera housing is shown in Figure 6.

Figure 5. Camera Housing with Thermocouples.

Total cost of the camera housing manufacture was $1533.50. This is in excess of the initial proposed cost, however it is still significantly lower than the cost of a premanufactured furnace camera.

Validation Testing

The high-temperature camera housing was tested at Southwest Research Institute's Department of Fire Technology on November 29, 2001. The camera housing was positioned in the wall of SwRI's Large Vertical Furnace used to test insulative wall assemblies. Validation of the camera design was conducted concurrently with an ASTM E119 fire resistance test of a wall assembly for an unspecified client. The temperature curve of the E119 test starts at ambient temperature and increases logarithmically to approximately 1500°F over the course of 30 minutes. In this instance the fire resistance test was carried out for duration of approximately 17 minutes.

Instrumentation

Before insertion through the furnace wall, the camera housing was instrumented with four Type K chromel-alumel thermocouples (TCs). The thermocouple locations are described in Table 4 and shown in Figure 5.

Table 3. Thermocouple Locations.

Number	TC Location
1	Front Viewport Cavity, 0.5 in. from glass surface
2	On outer surface, 2 inches from housing front
3	Inside exit water nozzle
4	Inside camera compartment

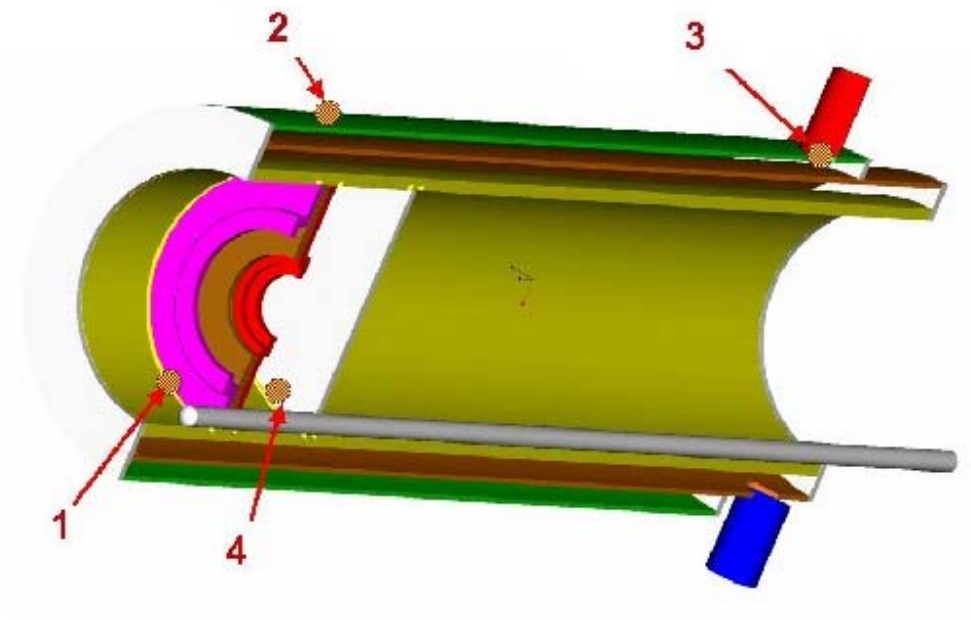

Figure 6. Thermocouple Locations.

Test Results

The furnace was ignited and run through the specified time-temperature curve for 17 minutes. Throughout that time, temperature within the camera compartment (TC 4) increased 2°C. Figure 7 shows the recorded furnace temperature curve and all recorded thermocouple data.

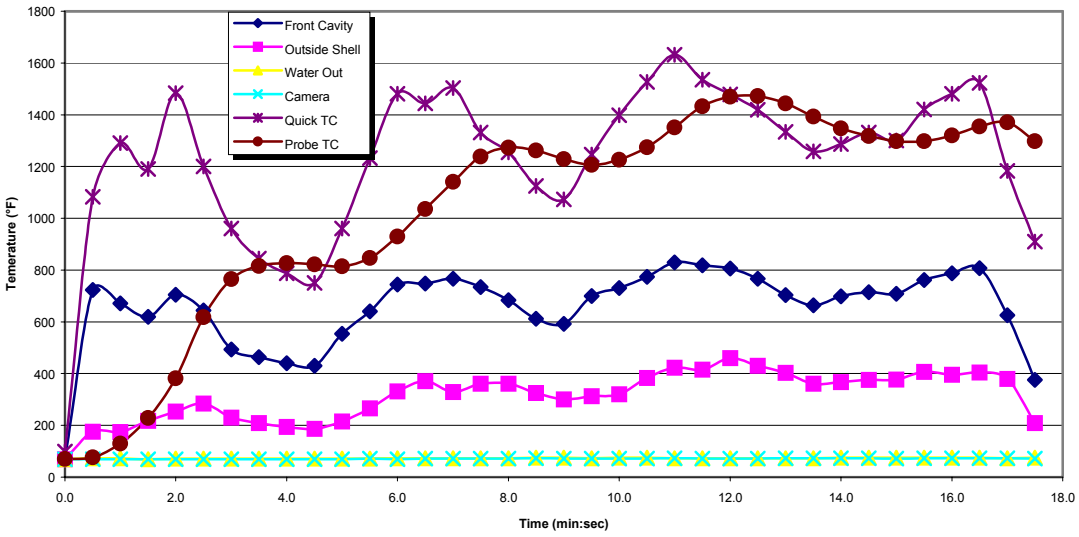

Figure 7. Recorded Temperature Data.

Throughout the course of the test, the camera operated as designed. Video was recorded without error and in relatively high definition. The furnace camera proved to be a valuable aid in test

observation by allowing clients and SwRI engineers to better understand the combustion characteristics of the test sample.

On conclusion of the test, data was graphed and analyzed. The peak temperature of TC 1, located in the front viewport cavity, was found to be higher than anticipated upon inspection of the recorded data. It was expected that the purge air supply would be sufficient to displace the hot air of the furnace, however the collected data shows that the flames of the furnace did penetrate into the viewport cavity. This is readily explained however, because the camera was by default mounted in direct line of a burner flame exhaust. Air velocity from the burner is more than sufficient to overpower the front air purge. Under this scenario, however, the housing functioned as designed in that the viewport assembly limited heat transfer to the inner camera chamber. The majority of heat introduced to the camera compartment was removed by the interior airflow around the camera.

The water-flow chambers functioned properly in their removal of the applied heat. It was noted that because the camera was mounted in the furnace wall insulation the heat load applied to the length of the camera housing was much less than specified in the design. The exposed surface of the camera, however, was directly impinged upon by flames from a furnace burner, creating a worse than anticipated heat load over the front end of the housing. Even though the exposed portions of the camera were in direct contact with the burner flame, the water transferred all heat applied to the assembly. At the conclusion of the validation test, the exit-water temperature increase was 3°C over initial.

From the measured water flow rate and the water temperature increase, actual applied heat can be determined. The calculated heat rate of 5279 W is approximately 20% of the heat application for which the housing was designed. This corresponds, however to the amount of exposed surface area of the camera inside the furnace. In addition, it is seen that while the furnace heat probes measured a maximum temperature of 1632 °F, the actual undiluted flames from the furnace at stochiometric composition are estimated to approach the anticipated 2000°F.

Conclusions

The camera housing met all design objectives. The view from the camera was better than anticipated and the increase in temperature in the critical camera compartment less than 3°C. Throughout the exposure, thermocouples verified that the camera was never in any danger from the furnace. Calculations proved to be reliable and were generally close to the actual measured values. It is recommended for future use that the camera be mounted further away from the line of fire of the burners to reduce direct flame exposure. The camera housing is currently located at Southwest Research Institute's Department of Fire Technology, where it is used for observation of test samples inside large-scale furnaces.

References

1. Incoprera, F.P. & DeWitt, D.P., Fundamentals of Heat and Mass Transfer, 5th Edition, August 2001, Wiley.
2. Reed, Richard. North American Combustion Handbook: Volume 1, Third Edition, 1986. North American Mfg. Co., Cleveland.
3. Underwriters Laboratories Inc. Standard for Safety. Rapid Rise Fire Tests of Protection Materials for Structural Steel. 1998. Northbrook.IL
4. American Standard for Testing and Materials. Standard Test Methods for Fire Tests of Building Construction and Materials. 1987. West Conshochochen, PA.
5. Moran, Michael J. and Howard N. Shapiro. Fundamentals of Engineering Thermodynamics, Third Edition. 1996. John Wiley and Sons, New York.
6. Fox &McDonald, Introduction to Fluid Mechanics 5th Ed.
7. Gere, James M. and Stephen P Timoshenko. Mechanics of Materials, Fourth Edition. 1997. PWS Publishing Co., Boston
8. Mills, Anthony F. Basic Heat and Mass Transfer. 1995. Richard D. Irwin Inc., Chicago.

DUSTIN M. GOHMERT

Mr. Gohmert currently is employed as a Flight Crew Engineer at United Space Alliance in Houston, Texas. He recently graduated from University of Texas at San Antonio in December of 2001 with a B.S. in Mechanical Engineering and has applied for graduate study at the University of Houston in the fall of 2002. Mr. Gohmert is currently an Engineer-In-Training and is pursuing professional registration in Texas.

PETER P. MEIER

Mr. Meier graduated in December of 2001 with a BS degree from the Mechanical Engineering Department at the University of Texas at San Antonio. He has recently moved to California and is currently looking for a full time position in Los Angeles.